

Comparative Analysis of ST-100 and ST-100M Hall Thruster Prototypes for Mission-Specific Applications

Dr. Dmytro Voronovskyi
*Department of ionized media
mechanics,*

*The Institute of Technical Mechanics of
the National Academy of Sciences of
Ukraine and the State Space Agency of
Ukraine*

Dnipro, Ukraine
<https://orcid.org/0009-0000-7893-3132>

Mr. Serhii Asmolovskiy
SETS (Space Electric Thruster Systems)
Dnipro, Ukraine
sergei.asmolovskii@sets.space

Dr. Bohdan Yurkov
*Department of ionized media
mechanics,*

*The Institute of Technical Mechanics of
the National Academy of Sciences of
Ukraine and the State Space Agency of
Ukraine;*

SETS (Space Electric Thruster Systems)
Dnipro, Ukraine
bohdan.yurkov@sets.space

Dr. Serhii Kulagin
*Department of ionized media
mechanics*

*The Institute of Technical Mechanics of
the National Academy of Sciences of
Ukraine and the State Space Agency of
Ukraine*

Dnipro, Ukraine
<https://orcid.org/0000-0002-2862-5809>

Abstract— This study provides a comparative assessment of the ST-100 Hall-effect thruster and its magnetically shielded counterpart, the ST-100M, designed to enhance longevity by minimizing channel wall erosion.

Erosion of dielectric channel walls remains a critical limitation for thruster operational life. The ST-100M incorporates an optimized magnetic topology, developed using ANSYS Maxwell simulations, to deflect ion flux from the walls. This design significantly reduces erosion but introduces trade-offs, particularly at lower propellant flow rates where reduced plasma density can impact ionization efficiency.

Comparative analysis confirms that the conventionally designed ST-100 is a cost-effective solution for shorter-duration missions. In contrast, the ST-100M, with its extended lifespan, is suited for long-duration applications such as station-keeping or deep-space exploration.

In conclusion, magnetic shielding in the ST-100M effectively mitigates erosion and enhances durability; however, performance optimization at low power is still necessary. The ST-100 remains viable for cost-sensitive missions, while the ST-100M is recommended for operations requiring prolonged service life and sustained performance.

Keywords—Hall thruster, magnetic topology, wall erosion, electric propulsion

I. INTRODUCTION

Over the past decade, the space industry has experienced rapid growth, primarily driven by a significant increase in the number of satellites in orbit [1]. The transition from single-satellite missions to large-scale constellations for communications, Earth observation, and other applications is fundamentally reshaping the utilization of near-Earth space [2].

In parallel, concepts of orbital infrastructure are actively evolving, particularly in the field of in-space servicing. These include debris removal, satellite maintenance, refueling, and orbital transfer services. Such systems are aimed at improving

resource efficiency and extending the operational lifetime of spacecraft [3-4].

The implementation of these concepts requires propulsion systems capable of delivering high total ΔV while maintaining high efficiency. In this context, electric propulsion systems, especially Hall-effect thrusters, are more suitable for long-duration missions compared to conventional chemical propulsion [5].

However, the operational lifetime of Hall-effect thrusters remains a key limitation, primarily due to the erosion of dielectric channel walls. Addressing this limitation is essential to meet the increasing demands of future space missions.

One promising approach to mitigating this issue is magnetic shielding, which reduces ion flux to the channel walls and, consequently, decreases erosion rates [6-16].

This study presents a comparative analysis of the ST-100 Hall-effect thruster and its magnetically shielded modification, the ST-100M with a power range of 800–1500 W. The results of experimental investigations of erosion zones on the dielectric walls of the discharge channel are presented.

II. MAGNETIC FIELD OPTIMIZATION

In this study, a design approach aimed at reducing erosion zones was applied to the 1.5 kW class ST-100 Hall-effect thruster developed by Space Electric Thruster Systems (SETS). The baseline configuration (Fig. 1) was first analyzed in order to establish a correlation between the magnetic field structure and the characteristics of erosion processes in the discharge channel.

The magnetic field distribution along the channel centerline was used to identify characteristic regions associated with erosion. The extent and position of the ionization and acceleration layer relative to the discharge channel exit are determined by the magnetic field parameters, including the magnetic field distribution and topology within the channel.

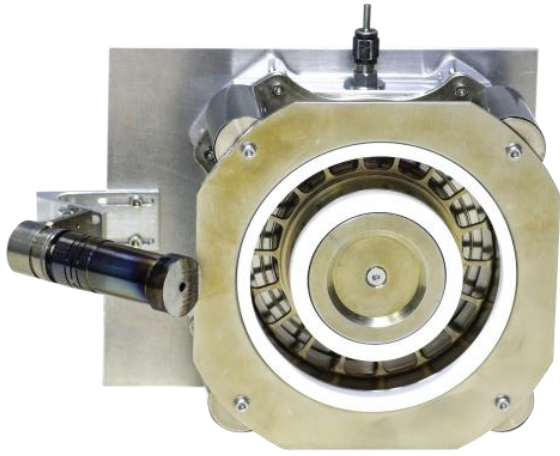


Fig. 1. General view of the ST-100 Hall thruster.

It is known that the ionization and acceleration layer is localized in the region of the discharge channel where the radial magnetic field reaches its maximum values. At the same time, the lower boundary of this layer corresponds to a position along the channel centerline defined by a value of $k \cdot Br_{\max}$, where k is a numerical coefficient and Br_{\max} is the maximum value of the radial magnetic field component. Known values of the coefficient k lie within a relatively wide range, from 0.6 to 0.9 [17]. At the same time, the position of the ionization and acceleration layer depends on the thruster operating regime, which is characterized by the discharge voltage and current.

The position of the erosion zone boundary in the discharge channel is directly related to the position of the ionization and acceleration layer and is determined by the geometric parameters of the thruster. The depth of the erosion zone, i.e., the extent of erosion of the inner and outer dielectric walls measured from the channel exit toward the anode, is generally different for the inner and outer walls of the discharge channel.

In most cases, the erosion depths of the inner and outer walls differ. In the present study, in order to reduce erosion of the inner wall, a magnetic field configuration with a diverging ion flux was implemented, in contrast to the conventional configuration, where the ion flux is focused toward the thruster axis.

To estimate the depth of the regions with increased ion-wall interaction, an empirical criterion based on the position of the point $0.8 \cdot Br_{\max}$ was employed. The predicted erosion zones, defined as the regions where these areas intersect with the discharge channel walls, are shown in Fig. 2.

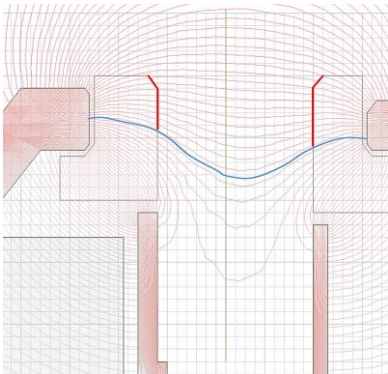


Fig. 2. Magnetic field line configurations and the predicted erosion zone in the discharge channel of the baseline ST-100 Hall thruster model.

According to the calculations, the erosion zone length is expected to be approximately 10 mm for the outer dielectric wall and 7 mm for the inner wall. To validate this approach, erosion zone measurements were performed after 120 hours of thruster operation. The experimentally obtained erosion zones (Fig. 3) indicate that the erosion zone lengths are approximately 11 mm for the outer wall and 7 mm for the inner wall. Despite the asymmetry between the inner and outer surfaces, the calculated and experimental results demonstrate satisfactory agreement in terms of erosion zone localization.

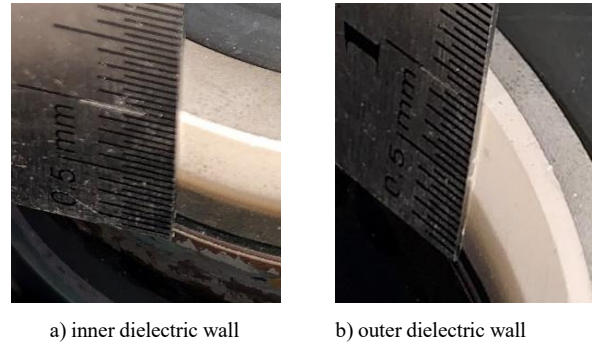


Fig. 3. Erosion traces on the inner and outer dielectric walls of the ST-100 discharge channel after 120 hours of thruster operation.

To reduce wall erosion by redistributing the magnetic field and modifying the discharge channel geometry, a magnetically shielded ST-100M thruster configuration was developed. In this configuration, the gap between the front face of the anode (magnetic shield) and the front face of the magnetic pole was reduced by 4 mm, and the ceramic pole pieces were extended toward the discharge channel exit.

The resulting magnetic field configuration provides partial magnetic shielding by aligning the profile of the dielectric channel walls with the magnetic field lines, thereby reducing the ion flux to the surfaces. It is important to note that the key geometric parameters and test conditions, including the mean channel diameter, laboratory feed system, cathode configuration, and cathode position, were preserved to ensure a valid comparison with the baseline design. The general view of the ST-100M thruster is shown in Fig. 4.



Fig. 4. General view of the ST-100M Hall thruster.

The predicted erosion zones for the ST-100M configuration are reduced to approximately 2 mm for the outer wall and 4 mm for the inner wall (Fig. 5).

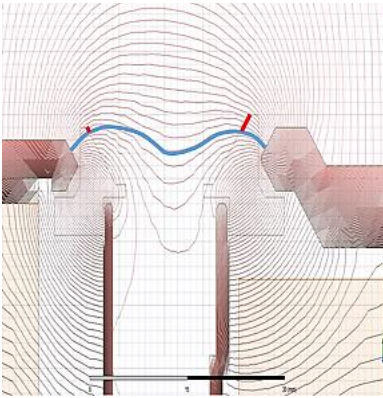


Fig. 5. Magnetic field line configurations and the predicted erosion zone in the discharge channel of the baseline ST-100M Hall thruster model.

The magnetic field distribution for the ST-100 and ST-100M configurations is presented in Fig. 6. Under identical coil current and winding conditions, in the baseline configuration the maximum of the radial magnetic field component is located approximately 1 mm downstream of the outer magnetic pole edge. In the modified configuration, this maximum is shifted to approximately 2.5 mm downstream of the pole edge. In addition, the position of the $0.8 \cdot Br_{max}$ point is shifted by approximately 3 mm along the channel axis.

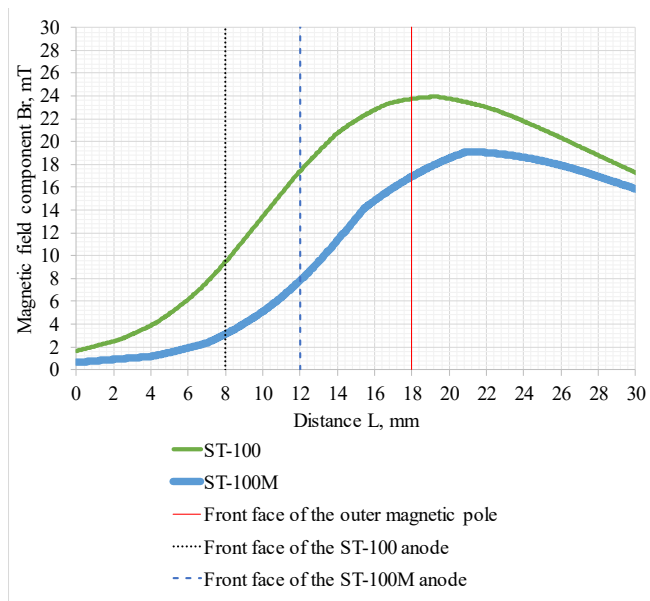
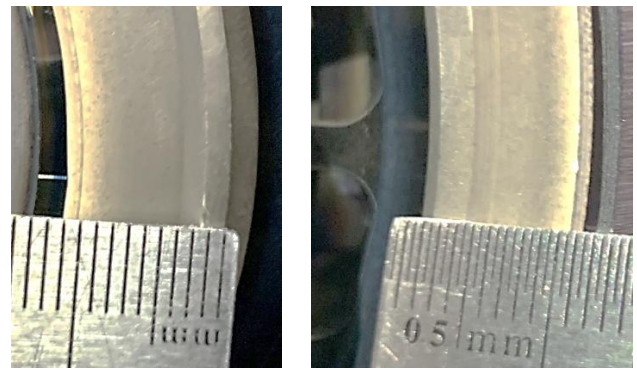


Fig. 6. Calculated values of the radial magnetic field component Br along the channel centerline for the ST-100 and ST-100M thrusters under identical coil current and number of turns. L denotes the distance measured from the anode toward the exterior of the thruster.

Experimental tests of the modified ST-100M thruster were conducted to evaluate changes in erosion zone length and performance characteristics compared to the baseline ST-100 configuration. Erosion traces on the discharge channel dielectric walls of the ST-100M are shown in Figs. 7. The observed erosion regions are approximately 1 mm on the outer dielectric wall and 1.5 mm on the inner dielectric wall.



a) inner dielectric wall b) outer dielectric wall

Fig. 7. Erosion traces on the inner and outer dielectric walls of the ST-100M discharge channel after 8 hours of thruster operation.

III. DETERMINATION OF OPERATIONAL PERFORMANCE

The vacuum chamber (Fig. 8) used for thruster testing was a cylindrical facility with a diameter of 1400 mm and a length of 3000 mm. The pumping system used for evacuating the test chamber and associated equipment did not employ oils or organic working fluids.

During thrusters testing, the chamber pressure did not exceed $2 \cdot 10^{-4}$ Torr, which was achieved using a turbomolecular pump with a pumping speed of approximately 4000 L/s for argon, supplemented by two cryopanels.



Fig. 8. Vacuum chamber for the Hall thrusters testing.

The results of functional tests of the ST-100 and ST-100M Hall-effect thrusters in the vacuum chamber are presented in Figs. 9–12 and show the dependencies of thrust F (mN), discharge current I_d (A), anode efficiency η (%), and anode specific impulse I_{sp} (s), from discharge voltage U_d (V).

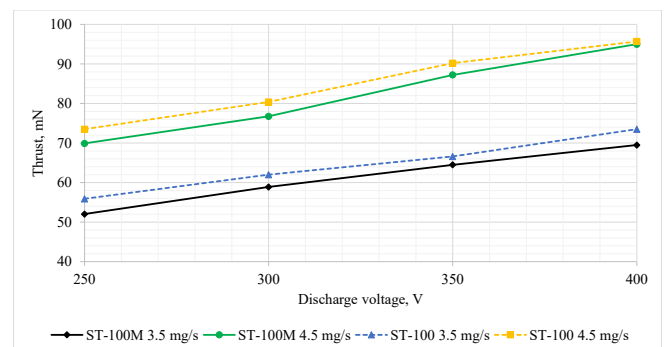


Fig. 9. Dependence of thrust on discharge voltage at different Xe mass flow rates.

V. CONCLUSIONS

The results of experimental investigations have shown that the modification of the magnetic system and the discharge channel geometry of the thruster made it possible to significantly (by approximately a factor of five) reduce the extent of the erosion zone in the discharge channel. This confirms the feasibility of developing Hall-effect thrusters with extended lifetime capable of meeting future mission requirements involving large dV .

However, it should be noted that this improvement is accompanied by a degradation of thrust and power performance characteristics (by up to 10%). Therefore, for missions requiring relatively short operational lifetimes, the conventional configuration without magnetic shielding may be more appropriate.

Further long-duration lifetime testing is required to validate these conclusions.

VI. FUTURE WORK

Long-duration lifetime testing is planned to determine the erosion rate of the discharge channel walls and to assess the actual lifetime of the ST-100M thruster. To enable precise erosion measurements at different stages of the lifetime tests, a dedicated measurement setup with a resolution of $1\ \mu\text{m}$ has been developed (Fig. 13).

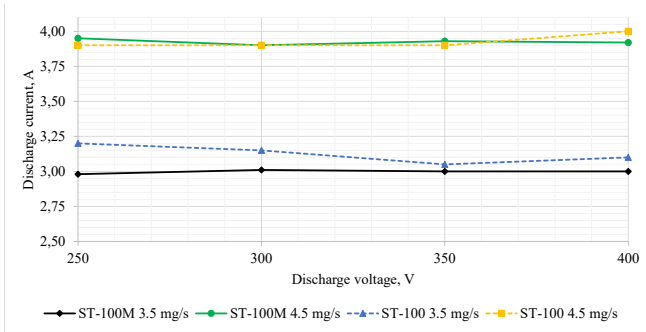


Fig. 10. Dependence of discharge current on discharge voltage at different xenon (Xe) mass flow rates.

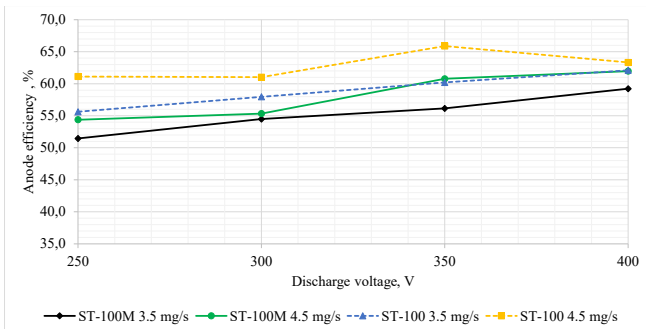


Fig. 11. Dependence of anode efficiency on discharge voltage at different Xe mass flow rates.

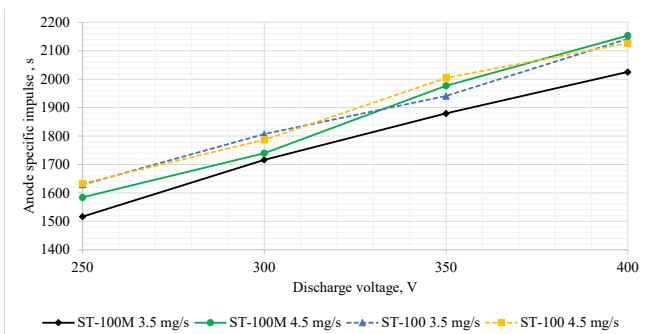


Fig. 12. Dependence of anode specific impulse on discharge voltage at different Xe mass flow rates.

IV. DISCUSSION OF RESULTS

As shown in Fig. 9, the thrust increases monotonically with increasing discharge voltage. A similar trend is observed for the anode specific impulse (see Fig. 12). The anode efficiency of the ST-100 thruster exceeds 65% at high-voltage operating conditions (Fig. 11).

As shown in Fig. 10, with increasing discharge voltage, the discharge current remains nearly constant, indicating efficient ionization of xenon.

The obtained functional parameters indicate that the modification of the thruster resulted in a reduction in thrust and a slight decrease in specific impulse, which is likely associated with the expansion of the discharge channel in the region of maximum magnetic field. This, in turn, led to a reduction in propellant utilization efficiency.



Fig. 13. Erosion measurement setup.

ACKNOWLEDGMENT

This publication is based on work supported by a grant from the U.S. Civilian Research & Development Foundation (CRDF Global). Any opinions, findings and conclusions or recommendations expressed in this material are those of the author(s) and do not necessarily reflect the views of CRDF Global. This support was related to the publication of this work and travel associated with its presentation.

The development and testing of the ST-100 and ST-100M thrusters, as well as all associated facility and experimental expenses, were fully funded and carried out by Fight Control LLC (trademark Space Electric Thruster Systems). The authors thank all company employees for their contributions to this work.

REFERENCES

- [1] G. Curz, D. Modenini, and P. Tortora, "Large Constellations of Small Satellites: A Survey of Near Future Challenges and Missions", *Aerospace* 2020, 7, 133. DOI:10.3390/aerospace7090133
- [2] J. Zhang, Y. Cai, C. Xue, Z. Xue, and H. Cai, "LEO Mega Constellations: Review of Development, Impact, Surveillance, and Governance", *Science & Technology*, Volume 2022. DOI:10.34133/2022/9865174
- [3] J. Mulvaney, D. Arney, C. Williams, J. Morel, C. Stockdale, C. Whitlock, and V. Balaji, "In-space Servicing, Assembly, and Manufacturing (ISAM) State of Play", NASA Langley Research Center, 2025 Edition.
- [4] In-space operations and services (ISOS), "An overview of EU-funded R&I projects supporting the development of ISOS capabilities", 2024. DOI:10.2925/3418140.
- [5] I. Öz and Ü. C. Yılmaz, "Design Tradeoffs in Full Electric, Hybrid and Full Chemical Propulsion Communication Satellite", *Sakarya University Journal of Computer and Information Sciences*, Vol. 2, No. 3, 2019. DOI:10.35377/SAUCIS.02.03.654206.
- [6] I.G. Mikellides, I. Katz, R.R. Hofer, D.M. Goebel, K. de Grys, and A. Mathers, "Magnetic Shielding of the Acceleration Channel Walls in a Long-Life Hall Thruster", AIAA-2010-6942, Proc. of 46th AIAA/ASME/SAE/ASEE Joint Propulsion Conference & Exhibit, Nashville, TN, USA, July 25 - 28, 2010.
- [7] I.G. Mikellides, I. Katz, R.R. Hofer, D.M. Goebel, and K. deGrys, "Magnetic Shielding of the Channel Walls in a Hall Plasma Accelerator", *Physics of Plasmas*, 18, 033501 (2011).
- [8] I.G. Mikellides, I. Katz, R.R. Hofer, and D.M. Goebel, "Design of a Laboratory Hall Thruster with Magnetically Shielded Channel Walls, Phase I: Numerical Simulations," AIAA-2011-5809, 47th Joint Propulsion Conference and Exhibit, San Diego, CA, July 31-Aug 3, 2011.
- [9] I.G. Mikellides, I. Katz, Numerical simulations of Hall-effect plasma accelerators on a magnetic-field-aligned mesh, *Physical Review E*, 86 (2012) 046703.
- [10] R.R. Hofer, D.M. Goebel, I.G. Mikellides and I. Katz, "Design of a Laboratory Hall Thruster with Magnetically Shielded Channel Walls, Phase II: Experiments", AIAA-2012-3788, 48th AIAA/ASME/SAE/ASEE Joint Propulsion Conference and Exhibit, Atlanta, Georgia, July 30-1, 2012.
- [11] I.G. Mikellides, I. Katz, R.R. Hofer, D.M. Goebel, "Design of a Laboratory Hall Thruster with Magnetically Shielded Channel Walls, Phase III: Comparison of Theory with Experiment", AIAA-2012-3789, 48th AIAA/ASME/SAE/ASEE Joint Propulsion Conference and Exhibit, Atlanta, Georgia, July 30-1, 2012
- [12] I.G. Mikellides, I. Katz, R.R. Hofer, D.M. Goebel, "Magnetic Shielding of Walls from the Unmagnetized Ion Beam in a Hall Thruster", *Appl.Phys.Lett.*, 102, 023509 (2013).
- [13] A.L. Ortega, I.G. Mikellides, R. Conversano, R.B. Lobbia, V.H. Chaplin. Plasma Simulations for the Assessment of Pole Erosion in the Magnetically Shielded Miniature Hall Thruster (MaSMi). 36th International Electric Propulsion Conference. 2019. IEPC-2019-281.
- [14] Wensheng H., Hani K., Daniel A.H. Variation in Ion Acceleration Characteristics of the HERMeS Hall Thruster during Magnetic Optimization. 36th International Electric Propulsion Conference. 2019. IEPC-2019-713.
- [15] P. Thoreau, J. Little. Influence of Field Topology on Magnetically Shielded Hall Thruster Performance. 37th International Electric Propulsion Conference. 2022. IEPC-2022-329.
- [16] Alejandro L.O., Ioannis G. M. Richard R.H. Lifetime Limitations in Hall Thrusters Operating at High Current Density. 39th International Electric Propulsion Conference. 2025. IEPC-2025-097.
- [17] J.A. Linell and A.D. Gallimore, "Statistical Analysis of the Acceleration Zone Location in Hall Thrusters", AIAA-2008-4721, Proc. of 44th AIAA/ASME/SAE/ASEE Joint Propulsion Conference & Exhibit, Hartford, CT, USA, July 21 - 23, 2008